

FAST, EXTENDED VELOCITY RANGE FLOW IMAGING BASED ON NONUNIFORM SAMPLING USING ADAPTIVE WALL FILTERING AND CROSS CORRELATION

W. Wilkening¹, B. Brendel¹, H. Ermert¹

¹Institute of High Frequency Engineering, Ruhr-University Bochum, Germany,

Abstract – Pulsed Wave Doppler (PWD) systems acquire an ensemble of N echoes per beam line at a constant pulse repetition frequency f_{prf} . The total time span determines the velocity resolution, and f_{prf} the unambiguous velocity range. The ensemble size N is by approximation inversely proportional to the frame rate, assuming that the system performs interleaving. For a given frame rate, a tradeoff can only be made between velocity resolution and velocity range. We propose a pulse sequence, a velocity estimation algorithm and an adaptive wall filter for nonuniform sampling, i. e. sampling with varying sampling intervals. This approach allows to increase the frame rate by increasing the velocity estimation error for high flow velocities.

INTRODUCTION

At present, it is accepted in the field of medical imaging that slow flow cannot be resolved when an ultrasound system is set up to image high velocities and that aliasing effects in bigger vessels have to be ignored when imaging slow flow.

More attention has been paid to this issue in RADAR, where theory for Doppler processing of non-uniformly sampled data has been developed, especially for multi pulse repetition time-sequences [1,2]. Such pulse sequences consist of subsets of pulse trains, where f_{prf} is constant within a subset but changes between subsets. A Doppler spectrum can be derived from the data by means of dealiasing and harmonic fitting strategies.

We propose pulse sequences and processing algorithms, where timing intervals may be chosen arbitrarily to meet the requirements of medical imaging. The velocity estimation is based on cross correlation, and the clutter filter is based on a spatially resolved velocity estimation for tissue and sample-wise elimination of the tissue flow component.

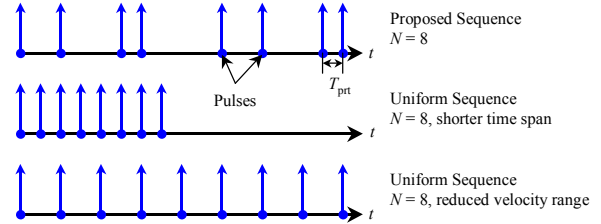


Fig. 1: Proposed nonuniform pulse sequence compared to sequences with the same ensemble size or the same time span, respectively.

PULSE SEQUENCE DESIGN

Assuming that depth and velocity estimation should be unambiguous, the maximum pulse repetition frequency depends on the maximum imaging depth z_{max} :

$$f_{\text{prf, max}} = \frac{c}{2 \cdot z_{\text{max}}}, \quad c = \text{speed of sound}. \quad (1)$$

Whenever $f_{\text{prf}} \leq 0.5 \cdot f_{\text{prf, max}}$, the time slot between 2 acquisitions for the same beam line is filled by acquisitions of echoes for other beam lines. This technique is referred to as interleaving. If we consider an ensemble with nonuniform sampling intervals, gaps of different sizes appear within the sequence and have to be filled in order not to sacrifice frame rate. We have designed a sequence consisting of $N = 8$ pulses, where the intervals are multiples of the shortest interval $T_{\text{prt}} = 1/f_{\text{prf}}$: $[2, 3, 1, 4, 2, 3, 1] \cdot T_{\text{prt}}$, illustrated in Fig. 1. This sequence and the time-reversed sequence can then be interleaved as shown in Fig. 2, where one slot per beam line remains free, but can be used to either acquire an echo for B-mode or to extend the sequence by one pulse: $[2, 3, 1, 4, 1, 1, 3, 1] \cdot T_{\text{prt}}$.

It is important for a nonuniform pulse sequence that many different intervals are represented in the sequence, and that multiple occurrences are distributed over the full time span. This improves the robustness

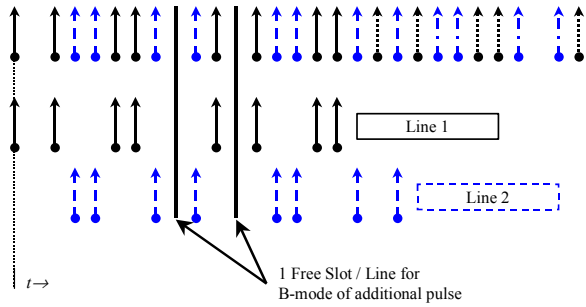


Fig. 2: The proposed pulse sequence is interleaving compatible. Free slots may be used for B-mode or to add one more pulse to the sequence.

of the velocity estimation, which will be discussed later. The proposed sequence fulfills this requirement as shown in Fig. 3.

VELOCITY ESTIMATION

Time-Shift Estimation

To estimate the velocity of a medium at a depth z , we first calculate the time shifts for all pairs of echoes in the sequences using cross correlation. $\binom{8}{2} = 28$ pairs representing time intervals in the range of $1 \dots 16 \cdot T_{\text{prt}}$ can be derived from the proposed sequence as illustrated in Fig. 3. To determine the time shift between the echoes of a given pair at a given depth, the cross correlation $c(\tau)|_z$ of the RF echoes is calculated for a range of time lags τ , where echo data is taken from two sliding windows symmetrically to the time t_z corresponding to the depth z . The procedure is graphed in Fig. 4. Typical window lengths correspond to $2\lambda \dots 4\lambda$ depending on the pulse length of the transmitted pulse and also on the SNR, where λ is the wavelength of the ultrasound pulse. The data in the windows may be Hanning-weighted.

As can be seen in Fig. 3, some time intervals are represented by several pairs, e. g. the interval $10 \dots T_{\text{prt}}$

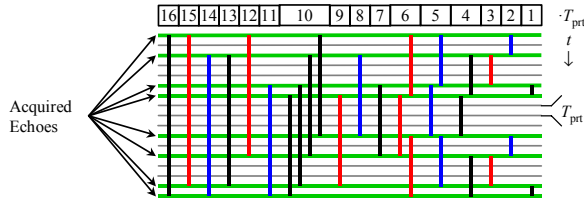


Fig. 3: Time intervals available in the sequence.

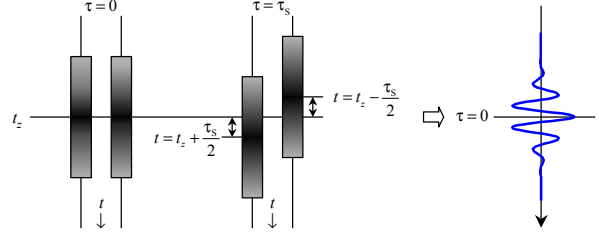


Fig. 4: The cross correlation function is calculated symmetrically to t_z applying sliding windows.

is represented by $k = 4$ pairs. Accordingly k cross correlation functions can be calculated. To combine the available information, a nonlinear approach was chosen, i. e. taking the maximum in k -direction:

$$c(\tau)|_z = \max_k (c_k(\tau)|_z) \quad (2)$$

The following reasons support this procedure: If the echo data in all k pairs are valid, the cross correlation functions are similar so that taking the maximum is equivalently useful as taking the mean. If in some pairs no strong scatterers are observed, which is in accordance with the inhomogeneous scatterer distribution in blood, $c(\tau)|_z$ represents noise and should not be taken into account. It may also be that strong scatterers move out of the sampling regions due to lateral or elevational flow components. In this case, the useful part of $c(\tau)|_z$ is taken and the rest discarded.

Cross Correlation

Once the cross correlation functions for the depth z have been calculated as described in Fig. 4 and (2), a set of cross correlation functions

$$c(\tau, n \cdot T_{\text{prt}})|_z, \text{ where } n = 1 \dots 16 \quad (3)$$

has to be evaluated. $c(\tau, T_{\text{prt}})|_z$ represent the shortest sampling interval and, therefore, defines the unambiguous velocity range. For simplicity, we assume a symmetrical velocity range. The allowed velocity range is conservatively chosen to correspond with a scatterer displacement of $\pm \frac{\lambda}{4}$ so that the velocity v is in the range of

$$-v_{\text{max}} = \frac{\lambda}{4 \cdot T_{\text{prt}}} < v < \frac{\lambda}{4 \cdot T_{\text{prt}}} = v_{\text{max}}. \quad (4)$$

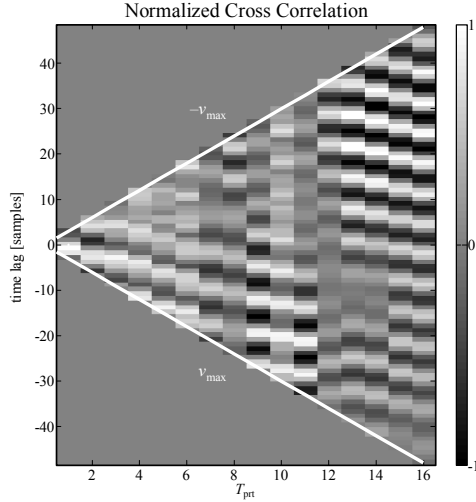


Fig. 5: Cross correlation as a function of time lag τ and time interval in multiples of T_{prt} . The allowed velocity range limits the correlation plane to the “estimation funnel”.

$c(\tau, T_{\text{prt}})|_z$ has consequently to be evaluated in the range of $-0.5 \cdot f^{-1} < \tau < 0.5 \cdot f^{-1}$, where $f = c \cdot \lambda^{-1}$. If we consider $c(\tau, n \cdot T_{\text{prt}})|_z$, the displacement by v will be scaled by n so that the range in which the cross correlation function is considered has also to be scaled to

$$-n \cdot 0.5 \cdot f^{-1} < \tau < n \cdot 0.5 \cdot f^{-1}. \quad (5)$$

Fig. 5 shows $c(\tau, n \cdot T_{\text{prt}})|_z$ for a velocity v within the allowed range. In this cross correlation plane, a velocity v is represented by a trajectory along maxima of $c(\tau, n \cdot T_{\text{prt}})|_z$ originating in $(\tau = 0, 0 \cdot T_{\text{prt}})$.

Velocity Tracking

Assuming that v is in the range defined in (4), it can be unambiguously determined by searching for the maximum of $c(\tau, T_{\text{prt}})|_z$. This estimation is also the most reliable one with respect to the fact that decorrelation noise will increase with increasing interval length, i. e. with increasing n .

Based on the initial estimate for v , the estimation is iteratively extended to increasing n . Moving from n to $n+1$ the “estimation funnel” (see Fig. 5) is narrowed to $\pm 0.5f^{-1}$ around the predicted τ_{n+1} , and the trajectory along which the sum of the correlation val-

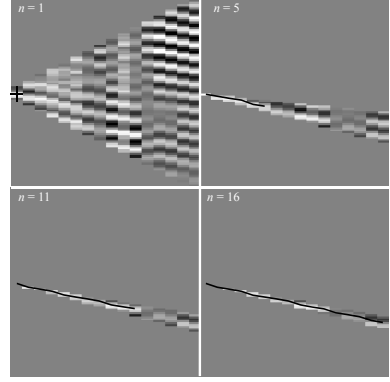


Fig. 6: Several steps in the iteration process of finding the trajectory corresponding to the flow velocity v within the estimation funnel, see Fig. 5

ues is maximal is then determined. The iteration for $n = 1, 6, 11, 16$ is illustrated in Fig. 6.

ADAPTIVE WALL FILTERING

The adaptive wall filter is based on a tissue flow estimation following the algorithm described above. The tissue flow component is then removed from the echo data. In the case that bigger blood vessels are in the imaging plane, the velocity estimation algorithm may estimate blood flow and remove the corresponding components from the data. To avoid this problem, the estimated flow velocity and the correlation values along the estimated trajectory are used to decide upon the observed medium. If blood is detected, the estimated flow velocity is replaced by the velocity of the surrounding tissue. A two-dimensional median filter is applied to the velocity estimates, which agrees with the fact that tissue is a contiguous medium.

The actual wall filtering is performed sample-wise: To compensate the tissue flow component of a sample, the mean of the sampled echoes is taken along a trajectory that represents the tissue flow velocity of

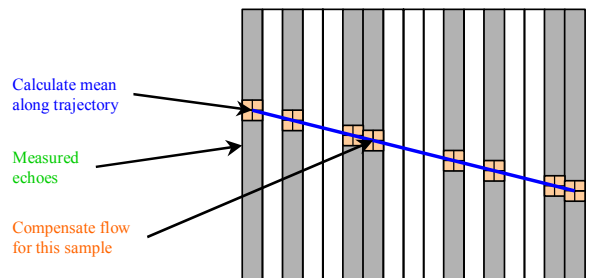


Fig. 7: Wall filtering is performed sample-wise by subtracting the mean along the estimated trajectory from the sample.

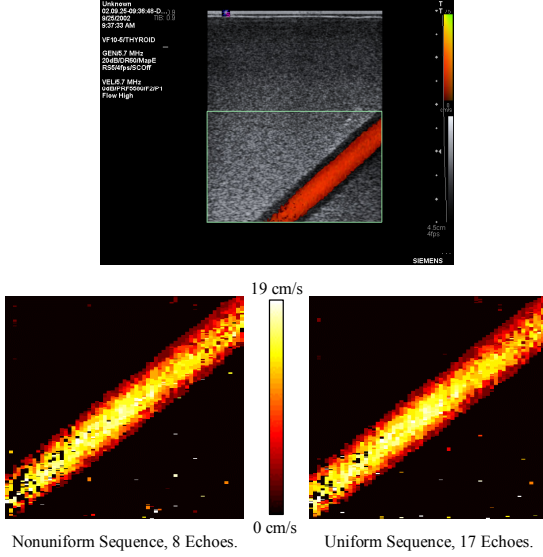


Fig. 8: Antares image (acquired at a higher flow rate). Flow images for nonuniform (8 Echoes) and uniform (17 Echoes) sampling calculated as described in this article.

that sample and runs through that sample. This mean is than subtracted from the very sample, see Fig. 7.

RESULTS

Flow Phantom

The algorithm was initially evaluated on a flow phantom. Data was acquired using a Siemens Sonoline® Antares equipped with a VF10-5 linear array. The transmit frequency was 5.7 MHz and the pulse repetition frequency was 5580 Hz. The ensemble size was $N = 19$. Out of this sequence, 8 echoes were selected to form the proposed nonuniform sequence. In comparison, a sequence of $N = 17$ echoes, thus having the same time span, was also considered. The results are summarized in Fig. 8. The tissue flow estimation yielded zero flow according to the fact that no motion artifact occurred during data acquisition.

In Vivo Data

In vivo data of a carotid artery was acquired using a Siemens Sonoline® Elegra with a 7.5L40 probe. The transmit frequency was 4 MHz and the pulse repetition frequency 4573 Hz. The results are visualized in Fig. 9. The tissue flow velocity was almost negligible.

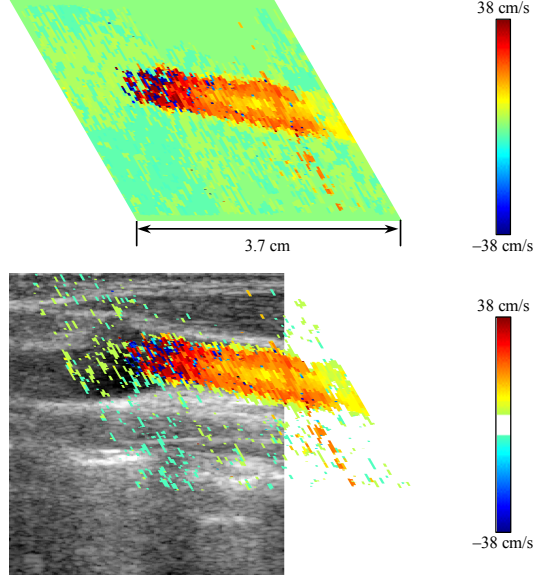


Fig. 9: In vivo image of a carotid artery. A nonuniform sequence of 8 echoes was taken from a uniform sequence with an ensemble size of $N = 20$.

CONCLUSIONS

We have proposed an nonuniform pulse sequence and correlation-based flow imaging techniques that enable flow imaging with reasonable relative velocity estimation errors over a wide velocity range. Adaptive wall filtering based on a tissue flow estimation was applied. In vitro and in vivo results prove the feasibility of the proposed algorithms.

ACKNOWLEDGEMENT

The work was carried out by the Ruhr Center of Competence for Medical Engineering (KMR Bochum), BMBF (Federal Ministry of Education and Research, Germany) grant 13N8079.

The authors would like to thank Siemens Medical Solutions for supporting the data acquisitions.

REFERENCES

- [1] E.S. Chorobay, M.E. Weber, "Variable-PRI processing for meteorologic Doppler radars," Proceedings of the 1994 IEEE National Radar Conference (1994), pp. 85-90.
- [2] Z. Banjanin, D.S. Zrnić, "Clutter rejection for Doppler weather radars which use staggered pulses," IEEE Transactions on Geoscience and Remote Sensing, vol. 29(4), pp. 610-620, 1991.